



# INFLUENCE OF THE FRACTAL LANDSCAPE IN THE FOREST FIRE PROPAGATION

BY  
FERNANDO J. AGUAYO FELLAY

ADVISOR  
PR J.P. CLERC AND DR A. FUENTES

SUBMITTED IN TOTAL FULFILLMENT  
OF THE REQUIREMENTS FOR THE COMPLETION  
OF THE MOBILITY GRANT AWARDED TO THE AUTHOR

AT  
INSTITUT UNIVERSITAIRE DES SYSTÈMES  
THERMIQUES INDUSTRIELS (IUSTI)  
UMR 6595 DU CNRS  
UNIVERSITÉ DE PROVENCE  
MARSEILLE, FRANCE  
JULY 2009

# Contents

<b>1</b>	<b>Introduction</b>	<b>2</b>
1.1	Percolation . . . . .	2
1.2	Fractal dimension . . . . .	3
<b>2</b>	<b>Fractal Surface</b>	<b>3</b>
2.1	FD determination: Box Counting . . . . .	4
<b>3</b>	<b>Percolation: A 3D example</b>	<b>6</b>
<b>4</b>	<b>Continuous fire spread model</b>	<b>8</b>
4.1	Models Assumptions . . . . .	9
4.2	Two-sites interaction . . . . .	10
4.2.1	Determination of the flux factor $f$ . . . . .	11
4.3	Self degradation . . . . .	14
<b>5</b>	<b>Numerical considerations</b>	<b>14</b>
<b>6</b>	<b>Simulations and numerical results</b>	<b>15</b>
6.1	Critical behavior . . . . .	15
6.2	Fractality . . . . .	18
6.3	Surface and $P_c$ . . . . .	21
<b>7</b>	<b>Conclusions</b>	<b>23</b>
	<b>References</b>	<b>24</b>
	<b>Appendix I: SCAT Presentation</b>	<b>25</b>
	<b>Appendix II: Personal Statement</b>	<b>38</b>

# 1 Introduction

The aim of the present work is to initiate a study of the effects of the landscape in the spread of forest fires. In order to do so we will need to clearly state the interaction rules between two neighboring trees at different heights. Although there exists different models for the wildland fires propagations, with different degrees of accuracy, we decided to start off with a novel approach that brings the flexibility and simplicity we required for the study. Thus we introduce a continuous (in time) spreading model for the fire propagation between neighboring sites, which we will use to understand the macroscopic properties of the system under different height scenarios.

We will mainly devote our attention to two principal concepts that will drive our interest. First, we will resort to *percolation* like systems to model the spread, as it is a simple yet complete description of the phenomena. Secondly, as way to use the model in a realistic scenario, we will use *fractal* surfaces to study the phenomena, provided we regard them as a good representation of natural processes and structures. But we will not be only interested in them as a surface-building procedure: we will also try to study the relation between this mathematical concept and the physical process.

## 1.1 Percolation

The forest fire spread is usually regarded as an example of percolation phenomena. In its simplest form, a mesh with occupancy probability  $p$  is used to represent the forest and the fire is introduced in this mesh allowing it to “infect” the nearest neighbors of a tree already on fire. In many physical systems this classical percolation picture is modified in very diverse ways, changing the spread mechanism, the way the mesh is constructed, the range of interaction, etc.

For example, in the case of forest fires, it is possible to find medium to long range interactions due to nature of the radiative heat transfer and/or spotting effects. These kind of interactions will affect the way the mesh is constructed: the links and their “weights” can be changed.

Another important effect to take into account in the forest fire spreading is the wind and topography of the terrain. This last one is particularly interesting in our case. Lets suppose we have an array of trees set on a terrain with certain slope. Clearly the fire will propagate easily to the higher terrain than downwards, not only that but it may be impossible for the fire to reach sufficiently deep terrain. This simple fact lead us to think that the process has some resemblance with the Directed Percolation (DP) kind of spread. In this scheme, the “infection” is possible only in some given direction which is in agreement with our notion of how the fire spread will behave. However, there are other important features that are not reflected in this model, as the fact that after a site has gone burned it is impossible to “revive” the site, to burn it again. This mechanism of reinfection plays a key role in the most well known DP schemes but is not present in our case of study. This immunization of site is nonetheless encountered in other kind of processes, known as “General Epidemic Process” (GEP). To be able to understand the interplay between the terrain and the fire spread will be of a great importance in our work, which intents to be a first step in the study of the impact of a fractal surface being used as the terrain where the mesh of trees lies.

Although the changes mentioned above, there is one characteristic that we want to keep from the classical percolation picture, that is the fact it exhibits a continuous phase transition between a self-extinguishing state and an infinite spreading one depending on the occupancy probability  $p$ . Below certain critical density  $P_c$  the fire will consume all the material within its reach and eventually starve to death, whilst above that threshold the active sites will always be within its reach. The behavior of the system close to that critical point can give us very important information about the system, namely it will allow us to identify the universality class at which the process belongs: Isotropic percolation (GEP is within this one), DP or some other class.

In next sections we will address the problem of how to introduce the dependency of the terrain in to the fire spread in order to understand how the fractal dimension of a given surface will be reflected in the measures performed in the fire evolution.

## 1.2 Fractal dimension

Fractal geometry is a relatively new branch of mathematics with roots in set theory, topology and theory of measures. This view is essentially different to the usual continuous representation of the nature. Most of the tools developed to tackle mathematical problems are made to work in a smooth world, but most of what we can measure in a forest, or any other natural system for that matter, is discontinuous and fragmented, and the typical tools are not mean for this. This is where the concept of fractality emerges.

Since Mandelbrot [1], who put fractals to the world's attention, powerful mathematical constructions have been used to understand and study the fractal world. Hausdorff-Besicovich measure of dimension, is one of the typical topological definitions that are used to characterize a fractal object. Normally one talks about the *fractal dimension*  $d$  of certain object, for they cannot be adequately described by usual 2 or 3 nor any integer Euclidean dimension,  $d$  is a fractional number. That kind of objects are usually found in self-similar constructions and in random patterns with several scales in their construction. This is the key to fractals, they are structures that possess more than one length scale, so they cannot be measured using only a straight line, because at each measurement step you will realize that the object has a even smaller structure that also has to be measured.

The most famous example of a fractal object is a coastline, full of twists and turns. Depending on the length of the “ruler” used to measure its length, you can get up to a 20% of difference, whenever you add more detail to the shore you get extra length in your total sum. And you can expect this to happen on measuring most of the irregular lines in nature, just think about smaller and smaller scales.

Here, we will try to use this concept to characterize and get more information about the process of fire spread. Although many aspects of a forest can be regarded as fractal, we will be interested in the particular role of the fractal surface that support the forest.

## 2 Fractal Surface

As we aim to understand the spread of fire and the importance of the fractal dimensionality on it, we will need to recreate natural-looking fractal surfaces in controlled way.

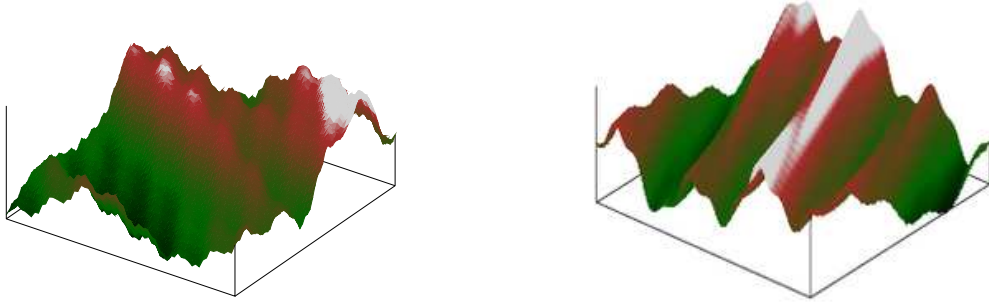


**Figure 1:** Fractal landscapes using random Weierstrass functions. (a) At the left  $d = 2.1$  and  $d = 2.2$  at the right (b).

Those kind of surfaces, in the literature has been largely generated [2] using Brownian surfaces, which tends to generate realistic random scenarios while its dimensionality is kept under control.

Starting from a mesh, or any set of points with some distance between them, the height of each point is given by the probability rule Eq.(1)

$$P(X(x+h, y+k) - X(x, y) \leq z) = (2\pi)^{-1/2} (h^2 + k^2)^{-\alpha/2} \int_{-\infty}^z \exp\left(\frac{-r^2}{2(h^2 + k^2)^\alpha}\right) dr, \quad (1)$$

where  $x, y$  is the position of a point,  $h, k$  is the distance in the respective axis and  $X(0, 0) = 0$  is enforced. Furthermore,  $\alpha$  is the index of the surface. The triplet  $(x, y, X(x, y))$  spawns the so called *index- $\alpha$  Brownian surface*.

The problems of generating a surface directly from Eq.(1) can be considerable. For these we resort to the use of a random Weierstrass function

$$X(x, y) = \sum_{k=1}^{\infty} C_k \lambda^{-\alpha k} \sin(\lambda^k (x \cos(B_k) + y \sin(B_k)) + A_k), \quad (2)$$

where the coefficients  $C_k$  are independent, normally distributed with mean 0 and variance 1.  $A_k$  and  $B_k$  are independent, uniformly distributed in the interval  $[0, 2\pi)$ . Although is not exactly a Brownian surface, it retains the principal statistic features and can be shown that  $\alpha$  controls the dimensionality in the same ways as in Eq.(1) [2]. Equation (2) is straightforwardly computable provided  $\lambda > 1$ , so the term becomes negligible at some  $k$ . Examples of constructed surfaces are depicted in Figs.(1)

## 2.1 FD determination: Box Counting

The Fractal dimension of an “object” is not unambiguously defined. Depending on the measure used different values can be obtained and still be in agreement with our

common perception. Furthermore different approaches can be related with different properties: Information content, Mass distribution, Geometry and others can be found in literature. In our case, as the geometry is the most important feature to investigate, we will use the Box-Counting method [2], which is strongly related to this aspect.

The concept behind is simple: in Euclidean space the volume  $V$  of an object scales as

$$V \propto L^d, \quad (3)$$

where  $L$  stands for the side of the object and  $d$  is its usual Euclidean dimension. Regarding this same concept as valid for fractional dimension, we proceed to discretize the object. For this we enclose the object in a “cube” of an Euclidean (integer) dimension  $d_E$ , above the expected one of the object. In sake of simplicity we assume the cube has side 1 to normalize the system. Then we divide the side of the cube in segments of length  $\epsilon$ , so the volume  $V$  will be directly proportional to the number of little cubes  $N_\epsilon$  of volume  $1/\epsilon^{d_E}$  needed to cover the object. So we get

$$N_\epsilon \sim 1/\epsilon^d \text{ as } \epsilon \rightarrow 0,$$

which leads to

$$d = -\lim_{\epsilon \rightarrow 0} \frac{\ln(N_\epsilon)}{\ln(\epsilon)}. \quad (4)$$

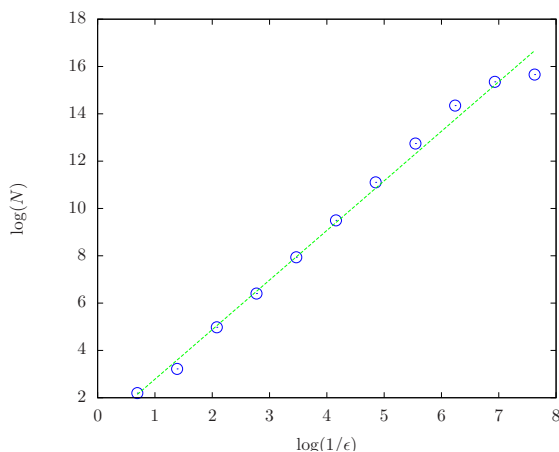


**Figure 2:** Number of used cubes as a function of the side length.

Of course this is only achievable for certain objects. In order to obtain  $d$  we compute the number of little cubes needed to cover the object for different small values of  $\epsilon$  and then, the slope of the curve obtained is regarded as the dimension of the object. Naturally, a straight line is not always obtained: only certain objects on certain scales behaves according this power law. When that behavior is found, one can say that “the object has fractal dimension  $d$  for this range of scales”. In Fig.(2) we can see how the curve  $\ln(N_\epsilon)$  v/s  $\ln(\epsilon)$  looks like for the surfaces (a) in Fig.(1). We can see how for large  $\epsilon$  it follows closely a straight line, but for smaller  $\epsilon$  it no longer has a well defined fractal (box) dimension.

Due to the random nature of the construction of these surfaces, it is possible to obtain an average of the desired fractal dimension as indicated in the Fig.(3) where the fractal dimension of the surfaces is plotted versus the parameter  $\lambda$ . Here the error bars represent the standard deviation of the sample.

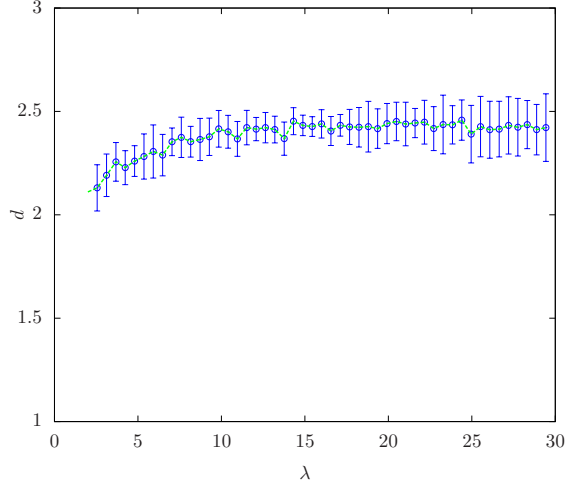


**Figure 3:** The curve represents the mean of the fractal dimension of the generated surfaces as function of  $\lambda$ .

### 3 Percolation: A 3D example

Before jumping into the problem of propagation in a fractal surface we will study an example of how additional dimensions plays a role in percolation. Although quite different than the extra dimensionality in a fractal dimension, this example will allow us to visualize how “reconnecting” the mesh in different way is reflected in the criticality of the phenomena.

The setup is simple: We will study the bond percolation (occupancy probability  $p$  is referred to bonds, not to the sites) in a 2D square mesh. The occupancy probability  $p$  inside of the mesh will be called  $p_{\parallel}$ . Next, we will put several of those meshes one above the other and will link the corresponding sites with a probability  $p_{\perp}$  forming a common 3D square mesh with 2 parameters, as shown in Fig.(4). The idea is to initiate the propagation on a complete side of this cube and measure at the opposing phase if the phenomena propagates through the cube.

This is repeated for several realizations so we can measure the “percolation density” for a given  $(p_{\parallel}, p_{\perp})$ . This quantity is plotted in Fig.(5).

The number of attempts that reaches the opposite side are almost 0 until the critical point and after the density is always almost 1. We will characterize this critical point as being the one where the maximum of the derivative is reached. For  $p_{\perp} = 0$  the critical point is identical to the one obtained in the typical bidimensional square lattice. But

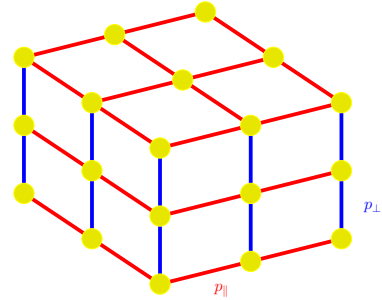


**Figure 4:** Representation of the cube: different colors in the links stand for different occupancy probability.

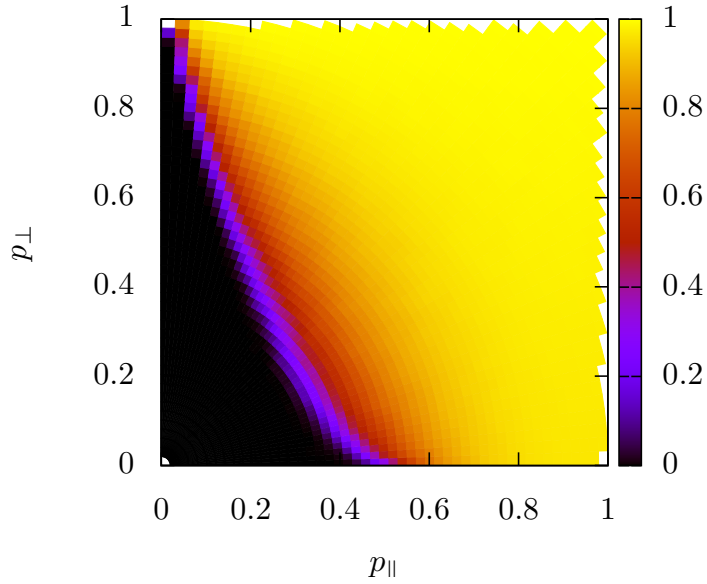


**Figure 5:** Map of the number of infinite clusters over the amount of realizations, for different configurations of  $p_{\parallel}$  and  $p_{\perp}$ .

as  $p_{\perp}$  increases this threshold decreases steadily until some minimum value is reached before some asymptotic behavior is observed. For this, is interesting to observe how the critical value  $p_c$  changes with the quantity

$$R = \frac{p_{\parallel}}{p_{\perp}}. \quad (5)$$

As we can see in Fig.(6) the percolation threshold decays with 2 different power law following the form:

$$p_c \propto R^{-\alpha},$$

depending the range of  $R$ : if it is greater or smaller than 1. We find that the best fit is given for  $\alpha = 0.51$  for  $R > 1$  and  $\alpha = 0.16$  otherwise. This means the extra ways in which the cube can be roamed from one side to another, decreases the percolation threshold with a given power law. Some questions that may arise are: How this behavior is modified in the case of a fractal surface? How randomness is reflected? Is the behavior at criticality also modified in some way? These question will treated in the followings sections.



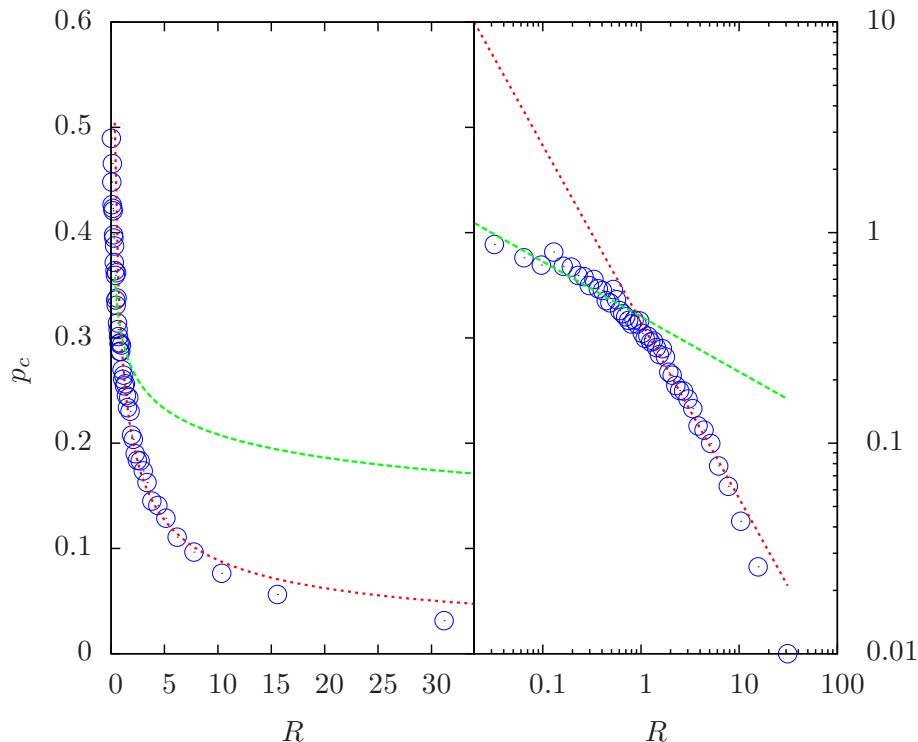


**Figure 6:** Behavior of the percolation threshold as function of the ratio  $R$ .

## 4 Continuous fire spread model

The following model allows to describe the spread of fire starting from the interaction between linked sites. Several models attempt to do so using percolation like processes in regular networks and cellular automata [3–6], giving different degrees of flexibility to the description. They usually define a computational procedure or some probabilistic rule to represent the spreading phenomena. In the present work, we start from a phenomenological description of the interaction between neighboring sites (trees) to construct the whole spreading process. This phenomenology is represented via a system of coupled first order differential equations for the normalized mass at each site.

We have adopted this continuous scheme instead of the more traditional discrete ones, as a way to perform a more systematic study of the involved parameters. Discrete models give a robust framework to understand the propagation phenomena, but when more effects are to be taken into account, a continuous representation seems more appropriate to represent all the underlying physics.

In particular, we focus our attention on the effect of the terrain height in the spread of a forest fire. As discussed in [7] and [8], these kind of contributions are essentially non-local, leading us to adopt a *local small world network (lswn)* approach to take into account the interaction further away than first neighbors. In the isotropic case, *i.e.* with no wind or slope, this construction leads to a system that can be regarded as a rank-1 network, which would enable to use the well known renormalization techniques (see *e.g.* [9]). In practice, the randomness of a real set-up, avoids us to do so. The

effects of the terrain will break the symmetry of the network, and even turning it into a directed graph because the propagation may be possible only in certain directions. This directionality will be local, highly dependant in the place the site occupies in the neighborhood. Furthermore, not only the topology will be affected, but also its links weight. The Experience confirms that the anisotropy induced by these agents also affects the dynamic properties of the system, as the velocity of spread [15]. Finally, the “microscopic” dynamic will also depend on the history of each site and not only on its current state, in the sense the ability of a site to infect its neighbors will change with time. For the above mentioned reasons, we propose a continuous spreading model over a *lawn*, which is spawned over the randomly occupied sites of a regular lattice.

The procedure to generate the network is as follows. A given regular lattice is filled with occupancy probability  $p$ , related to the density of the medium, in our case, the density of trees in a forest. For the occupied sites, the linking neighbors are to be found, in principle all the forest could be searched, but for computational convenience, in this work the neighborhood is comprised of all the active sites within 2.5 times the elemental mesh length. In Section 4.2 we will see that this is an adequate first approximation. Once the network and links are established the dynamics is controlled by the continuous spreading model.

## 4.1 Models Assumptions

In the following, we will assume the radiative heat transfer is the predominant mechanism in the propagation of forest fires. Although, convection can have important repercussions under certain circumstances, radiation has been shown to be the most important factor in propagation [15].

The state of the site is controlled basically by the evolution of the amount of fuel pyrolyzed. Moreover, this quantity is driven by different phenomena; ignition, burning rate and propagation. At the beginning, the decomposition of the solid fuel available in the tree (leaves, branches, etc.) is principally controlled by radiative heat transfer from a neighboring tree in flames. Once the solid fuel ignites, the self burning process will be the dominant phenomena (burning rate). Thus, we will study the two terms separately, each one in the absence of the other, expecting to describe the overall process in a reasonable way.

To adequately represent the propagation of fire between linked trees, we will start from the following set of rules:

- We will focus in the normalized fuel mass  $C_i(t)$ , relative to the initial amount of fuel in the site  $i$   $m_i^0$ , at time  $t$ . Thus,  $C_i(t) = m_i(t)/m_i^0$  so  $C_i(t = 0) = 1$  if  $i$  is active and 0 otherwise.
- $C_i=1$  and  $C_i=0$  are stationary states of the site if no external agent is considered.
- In order for a site to start the “self-combusting” process a minimal amount of incident radiative flux is needed.
- The radiation absorbed by a site is proportional to the amount of fuel left in that site.
- The degradation of a site is proportional to the energy received.

- When burning, the radiation emitted is proportional to the mass loss of a site.

## 4.2 Two-sites interaction

We state that, for a site  $i$  which neighbor  $j$  is burning,

$$\Delta C_i = \alpha E_j^r = \alpha E_j f(\mathbf{x}_i - \mathbf{x}_j) r C_i, \quad (6)$$

where  $E_j^r$  is the total amount of energy received in form of radiation coming from the site  $j$ . This quantity in turn is proportional to the total energy released  $E_j$ , where the proportionality factor is composed by the radiative energy portion  $r$ , usually about 35% [10], and a geometric view factor  $f(\mathbf{x}_i - \mathbf{x}_j)$ . The proportionality constant  $\alpha$ , is related to the heat of ignition of the site  $i$ . These two quantities will be discussed later. The term  $C_i$  in the RHS of Eq. 6 stands for the capability of the site to absorb radiation which is proportional to the density of fuel left in the site, considering it mostly distributed in the surface of the canopy. Should a volumetric distribution be considered more adequate, a power of  $2/3$  has to be used for the fuel density.

The total emitted energy, for a given period of time, can be simply estimated using the amount of burned mass, as

$$E_j = c_h m_j^0 \Delta C_j, \quad (7)$$

where  $c_h$  is the heat capacity of the fuel. This in 6 and taking an infinitesimal time period, yields

$$\frac{dC_i}{dt} = C_i \frac{dC_j}{dt} (\alpha f(\mathbf{x}_i - \mathbf{x}_j) r c_h m_j^0) = C_i \frac{dC_j}{dt} W_{ij}. \quad (8)$$

This simple term will be the responsible of the interaction between sites. To take into account the whole neighborhood, a summation over the index  $j$  is needed.

In order to ignite a tree is necessary to initiate the decomposition of solid fuel. This decomposition is possible when an external source generate energy heating the fuel (normally by radiation) and releasing fuel vapors or pyrolysis gases. Normally, the ignition of a solid fuel can be correlated to a critical mass flux of pyrolysis gases value necessary to reach the ignition. In this study the parameter  $\alpha$  can be readily estimated by measuring the total energy needed to ignite the tree ( $E_i^i$ ), and the critical amount of fuel at which the ignition occurs ( $C_i^{th}$ ),

$$\alpha = \frac{\ln(1/C_i^{th})}{E_i^i}. \quad (9)$$

The energy needed can be obtained via  $E_i^i = h_i m_i^0$ , where  $h_i$  is the heat of ignition of the given fuel. So we can write the coupling constant  $W_{ij}$  as

$$W_{ij} = \left( \frac{\ln(1/C_i^{th})}{h_i} f(\mathbf{x}_i - \mathbf{x}_j) r c_h \frac{m_j^0}{m_i^0} \right). \quad (10)$$

Finally, for the view factor  $f(\mathbf{x}_i - \mathbf{x}_j)$  is estimated considering a simple view factor between the tree with flames and the target (the neighboring tree) using the concept of solid flame [10]. In this study the source was adopted as cylinder (solid flame) emitting

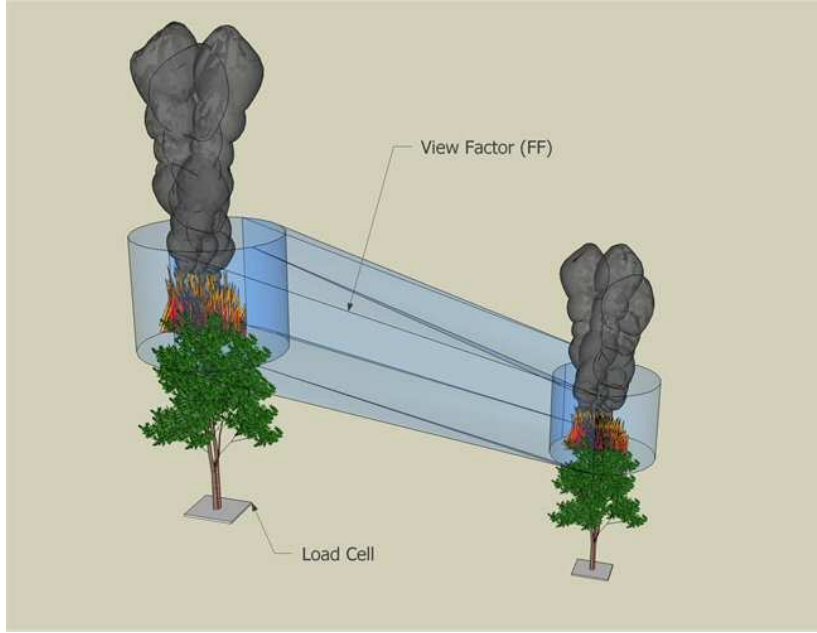


**Figure 7:** Schematic representation of the two-tree interaction.

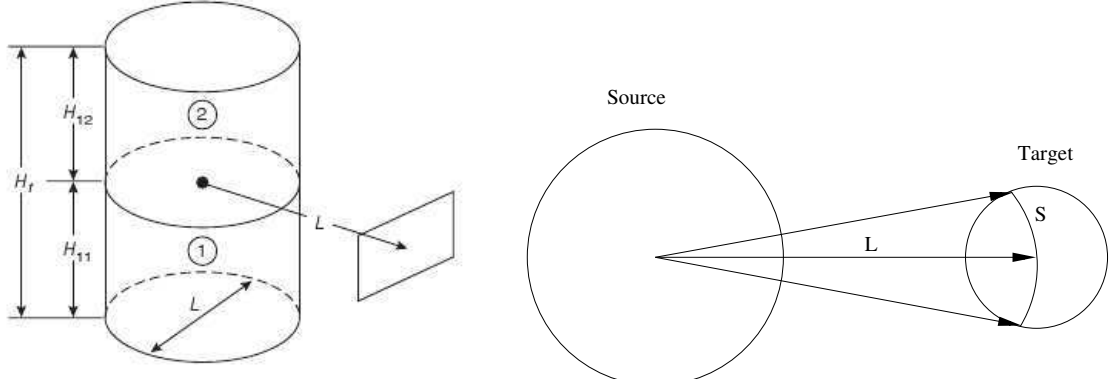
to a target (the neighboring tree) where is also a cylinder with or without the same dimensions. The radiation can be described then using analytical expressions of the view factors between a cylinder and a infinitesimal element of surface belonging to the target. A scheme of the set up is shown in Fig.(7). This geometrical consideration will impose a computational relief, as mentioned before in this section. The quadratic decay will allow us to neglect the interaction between distant neighbors, allowing us to keep the amount of links of each site in a small amount, but conserving the significant long range interactions. This *lswn* nature of the system makes the percolation threshold fall below 0.5, giving a sparse distribution at the phase transition, which will make the eventual “screening” between trees less important, and will not be taken into account in the calculations, as the critical behavior will be well represented.

An important final remark has to be done about this factor, as is here where the dependency in the surface is hidden. It relates the flux between two vertical surfaces (cylinders), so it will peak when both are vertically centered. As the surface representing the flame raises above the canopy, it will increase the propagation towards slightly higher surfaces and will produce a decreasing radiative flux for surfaces away from the center. This is the expected behavior and will drive the height dependency in the spreading model.

#### 4.2.1 Determination of the flux factor $f$

We take into account only radiation for the fire propagation. In the most simple scenario we consider the trees as cylinders emitting and absorbing radiation to and from their neighbors. Accordingly to [10], the radiation emitted by a source is given by the equation:

$$\dot{q}'' = EF_{12}, \quad (11)$$



(a) Scheme of the radiation received by a punctual target.

(b) *Superior* view of the schematic setup.

**Figure 8:** Scheme of the cylindrical view factor.

where  $F_{12}$  is the form factor for the specific shape. In our case, for a cylindrical source and a vertical target we have:

$$F_{12,V} = \frac{1}{\pi S} \tan^{-1} \left( \frac{h}{\sqrt{S^2 - 1}} \right) - \frac{h}{\pi S} \tan^{-1} \left( \sqrt{\frac{(A+1)(S-1)}{(A-1)(S+1)}} \right) - \frac{Ah}{\pi S \sqrt{A^2 - 1}} \tan^{-1} \left( \sqrt{\frac{(A+1)(S-1)}{(A-1)(S+1)}} \right),$$

where

$$\begin{aligned} A &= \frac{h^2 + S^2 + 1}{2S} \\ B &= \frac{1 + S^2}{2S} \\ S &= \frac{2L}{D} \\ h &= \frac{2H}{D}, \end{aligned}$$

and

$L$  = distance between the center of the cylinder to the target,

$H$  = height of the cylinder,

$D$  = cylinder diameter.

Using this model we can estimate the radiation received by a punctual target at a certain distance. To achieve that we use a scheme as in Fig.(8(a)).

Now, as our target is not punctual, but another cylinder we have to integrate over its receiving area. In order to reduce computation time and simplify the model, we take the simplified surface depicted in Fig.(8(b)). Then, the arc  $S$  is a portion of a circle of radius  $L$ , thus, orthogonal to the distance. With this, we only need to calculate the radiation incoming for one point, and knowing the length of the portion of arc  $S$ ,

namely

$$S = 2L \left( \pi - 2\cos^{-1} \left( \frac{r}{2L} \right) \right), \quad (12)$$

$r$  being the radius of the target, we only have multiply for this factor and then integrate in the height of the target to get the total incoming radiation. This last step is done numerically. The resulting radiation at different distances, as function of the difference

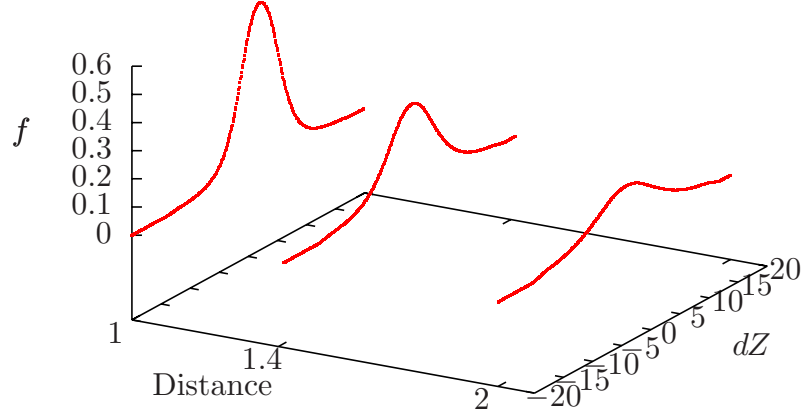


**Figure 9:** View factors at different distances for different heights of the target.

of height is shown in Fig.(9).

### 4.3 Self degradation

Once the decomposition process is started the mass pyrolysis rate is normally accelerated mainly by the radiation come from the own combustion processes carry out in the tree. Experimentally, this process shows a slow initial evolution if the canopy is ignited while still the moisture content is important. This is followed by an acceleration of the process in the intermediate stage and a new slow down at the end of the process, when the fuel has been mostly consumed [11]. For a burning tree, we purpose a mass evolution of the form:

$$\frac{dC_i(t)}{dt} = -C_i(t) (1 - C_i(t)) U_i, \quad (13)$$

which is in qualitative concordance with experiments [11]. For large times,  $C_i(t)$  will decay exponentially, relating the factor  $U_i$  to the inverse of the *mean-life* of the isolated burning tree, normally about 30s [16].

With this, the overall equation for the rate of mass over time of every active site is

$$\frac{dC_i(t)}{dt} = C_i(t) \sum_{<j>} \frac{dC_j(t)}{dt} W_{ij} - \Theta [C_i^{th} - C_i(t)] C_i(t) (1 - C_i(t)) U_i. \quad (14)$$

In Eq.14, the sum in  $<j>$  is to be performed over all the *burning* neighbors of  $i$ , as we only account for radiative processes. It is important to note that the second term in RHS is activated when the burning threshold  $C_i^{th}$  is reached.

## 5 Numerical considerations

From the computational point of view, the system is solved using a little of object oriented programming, creating a class for the sites with the necessary fields to store the relevant information such as position, an index number to order the trees in the forest, the amount of fuel left in the site, the received radiation in the two previous time steps and the index of the trees at which the site can radiate, to name some. In case of inhomogeneous vegetation (not used in this report) the physical quantities related to  $W_{ij}$  and  $U_i$  should also be stored here. Together with that information, methods capable of searching for the neighbors of the site and advancing one time step for a given configuration, are also implemented.

The numerical approach to perform this last task is using the simple predictive method *Adams-Bashforth 3*. This way the system of coupled first-order differential equations can be solved without requiring the radiation received in the current time step. This is a great advantage over other methods, since this quantity itself has to be determined, as it depends in the derivative of the mass density of the neighbors. Other possible approach is to iterate until convergence is reached, but due to the numerical intensiveness of such a process to be made over a large net we will not try this here, and stick to the most simple and fast method, which has a reasonable degree of accuracy.

The method solves

$$y' = f(y, x) = F(x), \quad (15)$$

using the relation

$$y_{n+1} = y_n + \frac{h}{3} (3F_n - F_{n-1}) + \mathcal{O}(h^3), \quad (16)$$

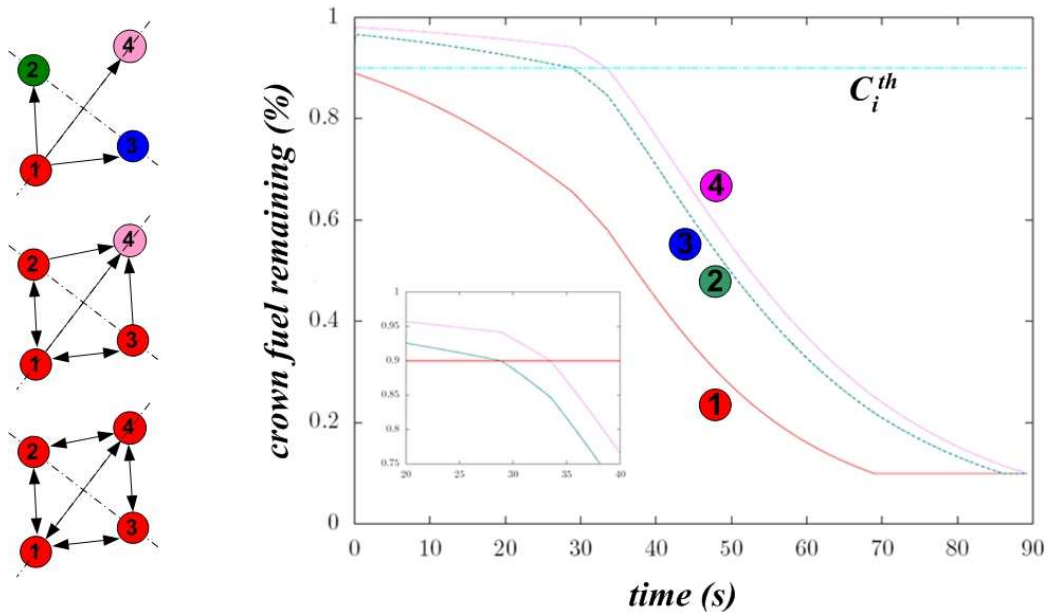


**Figure 10:** Simple interaction example of four trees. At the left a schematic representation. At the right the fuel available in each site in function of time.

for a time-step  $h$ . The value of  $F_n$  and  $F_{n-1}$  can be easily obtained from Eq.(14) at each time step.

Once the parameters are fixed and the solver implemented, is interesting to look the simple interaction between four trees, starting the simulation with one burning site (tree 1). The graph in Fig.(10) shows that two sites that are identical (trees 2 and 3) because of the symmetry of the problem and only three curves are observed. There is an evident change in the slope of the curves when any of them reaches the ignition threshold  $C_{th}$ . In the one hand the self burning process accelerates the degradation, and in the other, this process also contributes to increase the slope for the fuel mass losses evolutions of the neighboring trees.

## 6 Simulations and numerical results

We now turn to the application of the model to study the dynamics of the system. First, we will study the behavior and then the idea is to compare the results against the ones obtained using other models, which describes the phenomena. We will be interested in recreating the phase transition that separates the propagative and non-propagative regimes and in obtaining physically reasonable dynamical quantities. After the validation of the model we will study the impact of the fractal landscape in the propagation of fire.

### 6.1 Critical behavior

We aim to study the second order phase transition, usually present in this kind of systems. The system is simulated over a square lattice for different configurations of



the landscape. The most simple case consist in a flat surface with different inclinations, ranging from 0 to twice the optimal propagation height given by  $f(\mathbf{x}_i - \mathbf{x}_j)$ . To study the spread in wildland forest fire we also simulate using a randomize Weierstrass surface of several fractal dimensions [2], which are usually regarded as “realistic” scenarios. The runs starts as a single seed in the center of the mesh and are stopped when the fire reaches the border of the mesh (the boundaries of the domain) or when the fire stops spreading. In this way size effects are irrelevant. To study the criticality we measure the survival probability  $P_s(t)$ , the number of active sites  $N(t)$  and the mean square radius of the infected zone measured form the origin  $R^2(t)$ . Those quantities are averaged over all surviving runs. Is reasonable to expect a behavior at the critical point as [12]:

$$P_s(t) \sim t^{-\delta}, N(t) \sim t^\theta, R^2(t) \sim t^{2/z}. \quad (17)$$

The dynamical study of the critical behavior best suits this particular configuration, since other quantities like correlation length or cluster size lost their meaning in a directed network.

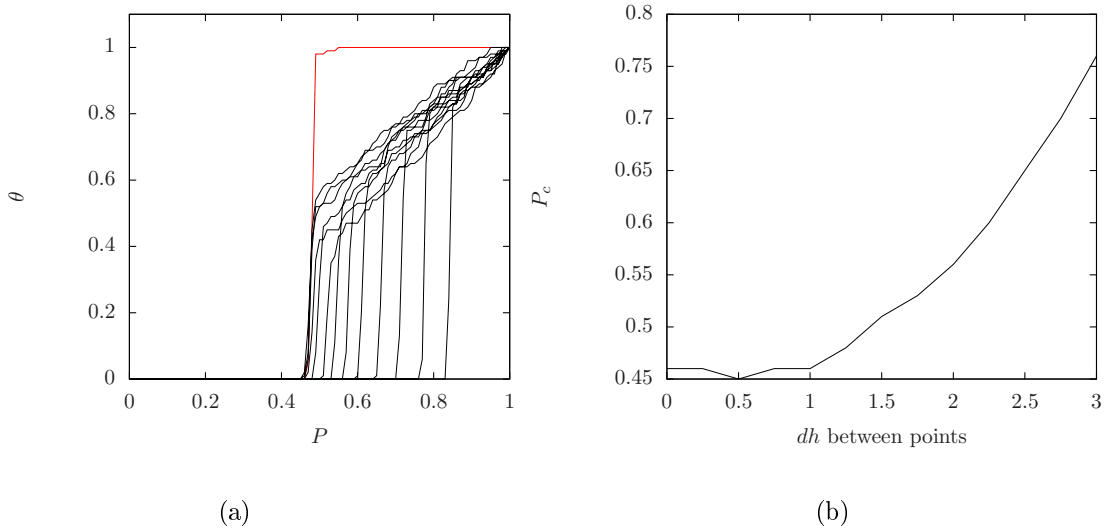


**Figure 11:** (a) The percolation density for different inclinations. (b) the percolation threshold as function of the slope.

In Fig.(11(a)) the percolation density is shown for flat surfaces with different inclinations. The red curve represents the results for no inclination and the black lines represent surfaces ranging from 0.25 to 3 m of difference between closest neighbors (the mesh distance is 5 m). For the horizontal plane the phase transition is very abrupt, but adding just a little positive slope of the surface generate a behavior much smoother. In Fig.(11(b)) the evolution of the percolation threshold is plotted versus the slope. As for larger height differences the radiative processes becomes weaker. The increase in the slopes generates an increment in  $P_c$ , having a minimum close to 0.5 m. This distance is much smaller than the one at which the higher flux between closest neighbors is found (which is around 2 for this study, see Fig.(9)). We relate this fact to the importance of the propagation to the downward direction and to the long range interactions. Both

processes are benefited by smaller slopes. While only closest neighbors interactions takes the advantage of higher inclinations. This result shows that even when fires in hills can spread faster, it may be more difficult for them to spread to larger areas, provided the density of vegetation is smaller than the percolation threshold.

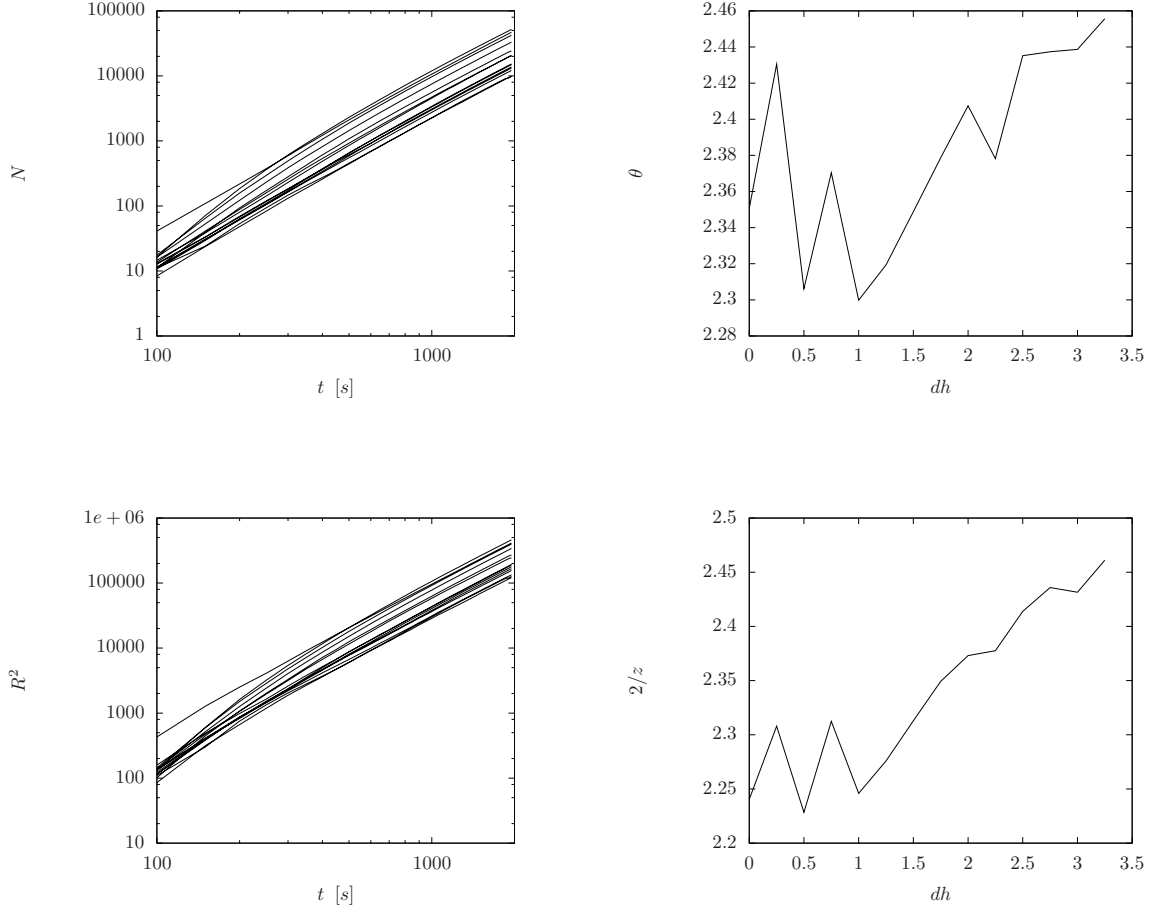


**Figure 12:** Figures of  $N$  and  $R^2$  at criticality and their critical exponents.

The interesting quantities of Eq.(17) are shown in Figs.(12) at the critical point. Both,  $N$  and  $R^2$ , shows a power law behavior for large times, but growing faster at early times. This change in the propagation rate is probably induced by the acquisition of a critical mass and could provide an interesting subject for future work. It has some intriguing resemblance with the results given in [12], in an interplay between DP and GEP.

The critical exponents shown by these curves are greater than the ones reported in the literature for GEP or DP, but this result has to be read carefully, since the quantities studied here have physical dimensions, unlike most of the other, more computational, systems. A little more effort is needed to take these results to some adimensional parametric forms using the natural time and length scales,  $U_i$  and mesh distances respectively. The growing behavior of the critical exponent as a function of the slope,

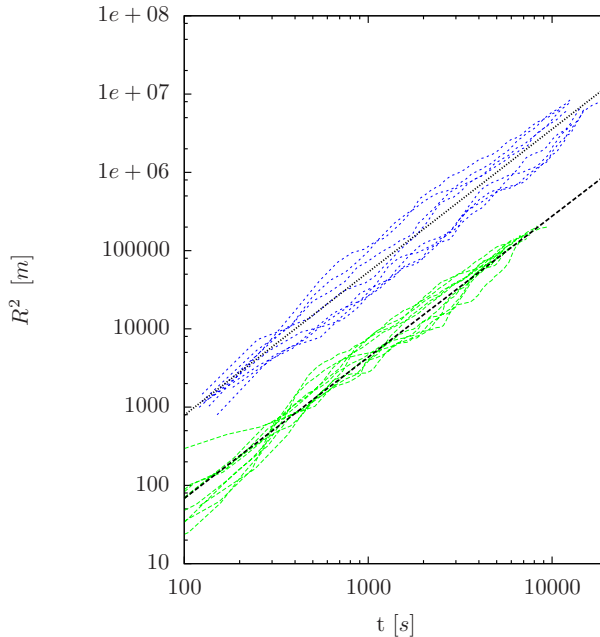


**Figure 13:** Critical behavior of  $R^2$  for different fractal surfaces, at 2 different mesh sizes (shown with offset).

is related to the increment of the percolation threshold. This rise in the available fuel produces a bigger cluster, capable of reach or propagate towards a larger amount of sites at each time step, which produces greater critical exponents.

In Fig.(13) the mean square radius of burned sites versus time for a series of fractal surfaces is shown for two different mesh sizes, one (blue) the double of the other (green). Although the existence of an appreciable dispersion of the data, the mean curve (not shown in Fig.(13)) follows closely a power law of the form (17), with exponent  $\frac{2}{z} \sim 1.8$ , in agreement with that of [13] for GEP in a two dimensional lattice (but again, has to be read with caution).

## 6.2 Fractality

Starting from the above mentioned initial conditions we will measure the fractal dimension of the active sites, the fire front and the active sites left in the mesh, for several realizations for different surfaces. Plots of the evolution of those quantities are shown in Fig.(14).

In the left column is shown the evolution of the dimension with time for different occupancy densities, ordered vertically in increasing order from 0.1 to 1.0, for 4 realizations. The excerpt graph, shows the number of sites versus time for the doping with longer survival time (closer to  $P_c$ ). In the right column we plot the evolution of the dimension for the density closer to criticality.

**Dimension of the Active Sites** The dimension of the active sites remains almost constant during the whole process. It normally starts nearly to  $d = 2$  (the fractal

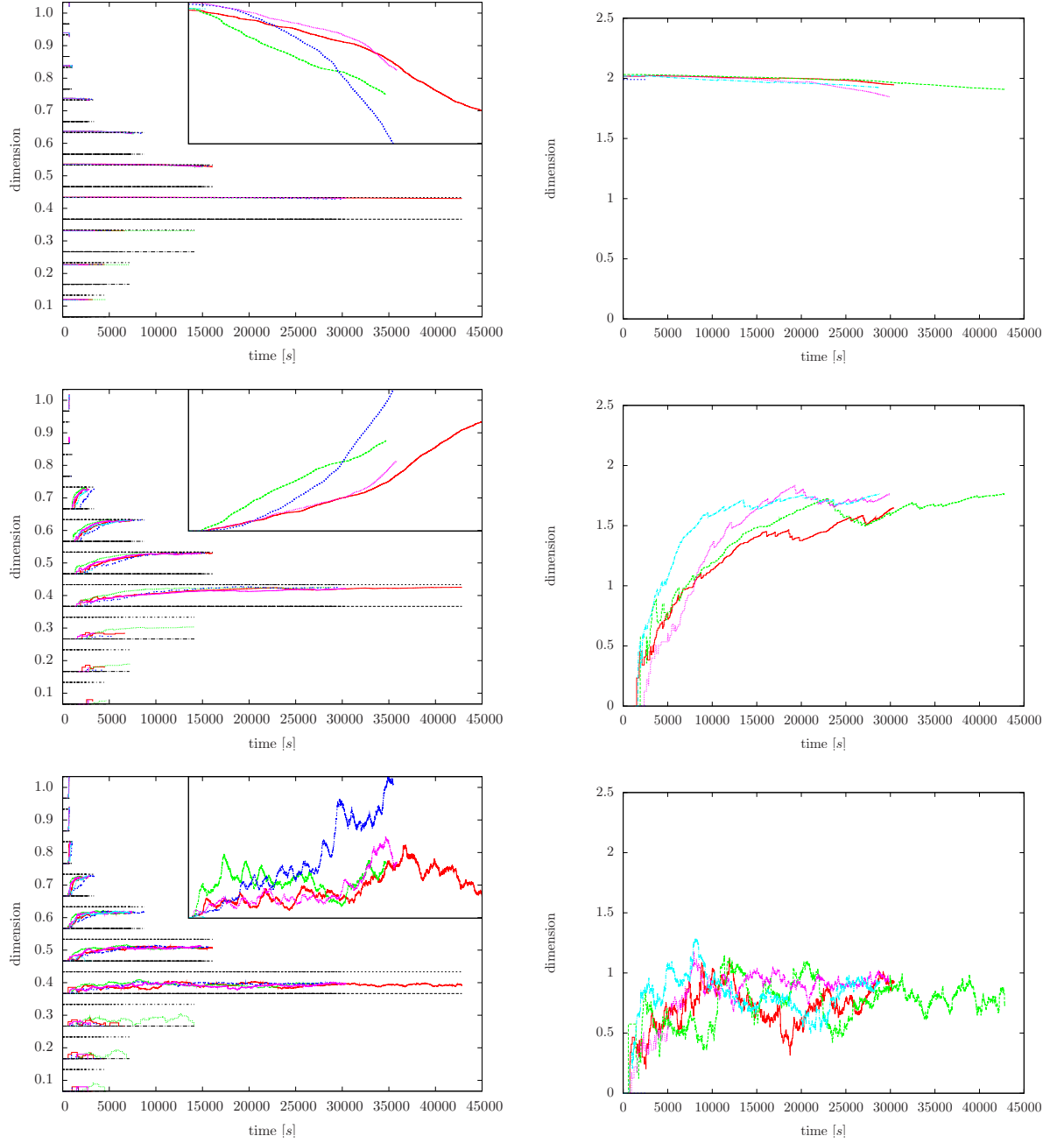


**Figure 14:** At the left the fractal dimension of the active, burned and burning sites for several occupancy densities. At the right a detailed view for the density closer to the percolation threshold.

dimension of the surface), and decreases when the doping is higher than the percolation threshold, while for lower doping it remains constant. It is interesting to note that although the dimension of the active sites doesn't go to 0 as in the flat case (above  $P_c$ ), it still varies, giving an estimation of the importance of the burned area.

**Dimension of the Burned Sites** The dimension of the burned sites starts from 0 and rapidly increases to 2. For larger meshes has been observed dimensions of the burned sites even going higher than 2 until reaching the dimension of the fractal landscape. It has been suggested [14] the way the dimension goes to the fractal surfaces dimension, may have a polynomial behavior related to some critical exponent. This was not approached in this work and will be a subject of research in the group in the near future. For example looking the relation between the dimensionality of the process with the critical behavior of the model.

**Dimension of the Fire Front** It starts from 0 (single point) and rises towards a constant plateau until that the fire front reaches the border. The dimension *plateau zone* seems to be independent of the surface dimension, and only depends of the doping. For a density close to the percolation threshold the dimension is close to 1, *i.e.* the fire propagates like a line whilst for higher doping the fire front grows close to 2. Again it has been observed that under particular circumstances the dimension of the fire front can grow above 2.

An important point is that above  $P_c$  the dimension seems to have recurrent patterns and a well defined global behavior. We would like to study how are they related to the fractal landscape. Also, the number of sites in the fire front as a function of time has stochastic behaviors over the well defined curve. Is there a relation between the fractal dimension of the surface and the distribution or “noise” in the curves? Other important feature is the dependency of the evolution on the initial condition. Upon a change in the selected ignition point, what remains in the description and what is lost, may give us some clues about the importance of the dimensionality over the mere topological features of the terrain. Finally, we can observe how the number of sites (shown in the excerpts graphs) behaves differently at a same density. While for one surface it has concave curvature for other surface is convex, showing us that they are in different phases (propagation and non-propagation). An interesting study will be to compare the behavior at the critical point of *each* surface.

### 6.3 Surface and $P_c$

In the preceding sections we studied how the “percolation” concept of the process is modified as the percolation threshold is no longer defined as a global quantity. In fact, it depends in the surface: for the same density the relevant curves (see Fig. (14)) have different behaviors, resembling those of sub and super critical regions. Therefore we can draw some conclusions: the randomness of the surface introduces a spread in the critical point. We still can see a second order phase transition separating the die-out and eternal-spread phases, but that transition will no longer be the same for all the realizations. To illustrate this point, in Fig.(15) we plot the percolation threshold versus

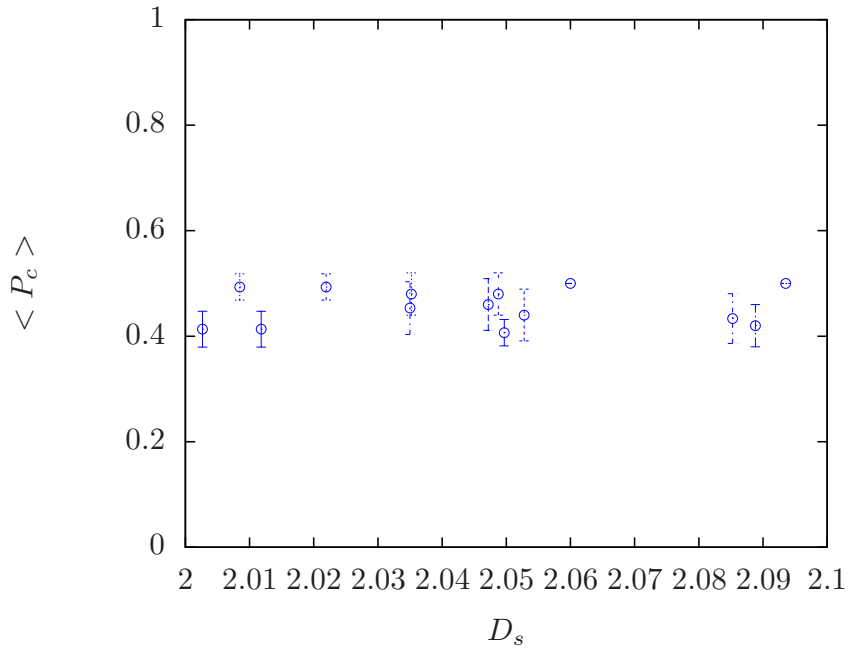


**Figure 15:**  $P_c$  for different surfaces, with different fractal dimensions.

the fractal dimension of the surfaces. The procedure is the following: given a surface a realization of the doping is made and its threshold calculated. Several realizations gives the mean percolation threshold for that surface ( $\langle P_c \rangle$ ) and its deviation is drawn as the error bars.  $\langle P_c \rangle$  does not seem to have a direct relation with the surface dimension, but we can see how its value changes from one surface to another, and from one realization in a given surface, to another. One question remains open: We now know  $P_c$  is very susceptible to the realization, but, what happens with the critical behavior of the system? Is there also a change or may it remain universal even when  $P_c$  is different?

In Fig.(16) we plot the mean survival time of the fire spread. Even when the critical point is at different places (reflected as different heights in the top of the curve) the way the curve behaves makes us think that the exponents are universal. Is necessary to note that after the criticality the mean time goes back to 0, this is due to the finite size of the system. So the left side of the graph surface only reflects how fast the fire reaches a border of the forest.

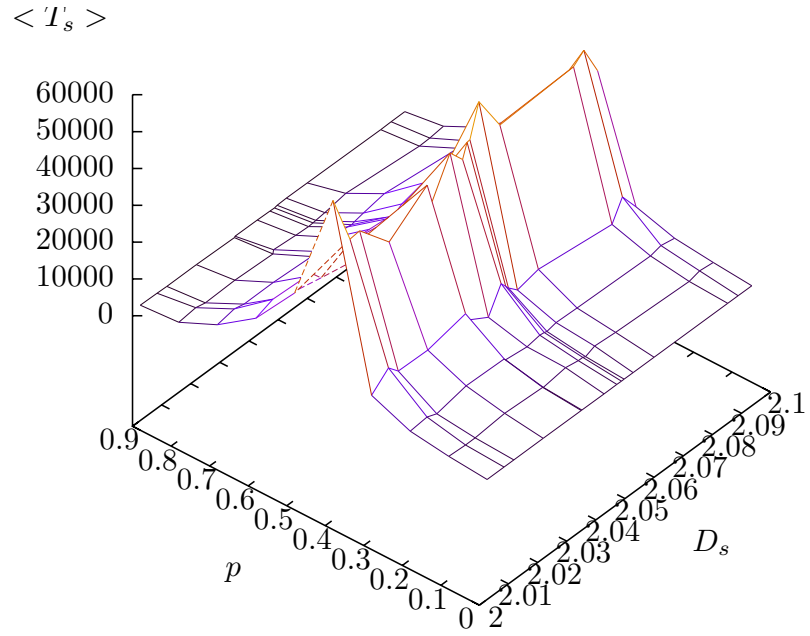


**Figure 16:** Survival time in function of the density and the surface fractal dimensions.

## 7 Conclusions

We have developed and tested a new model for the fire spread. The model is controlled by a phenomenological dynamics and is able to reproduce realistic spreading scenarios. It can include different types of vegetation and moisture conditions, as well as changes in the topography, being this last one the topic studied in this work. The changes in the surface are introduced via geometric factors that enters as parameters in the dynamic equations, giving a simple starting point to future studies and giving the possibility to introduce new effects, as the wind, in the description.

The model was used to simulate the fire spreading process in different surfaces for a fixed kind of vegetation. For flat surfaces with slope, the percolation threshold shows an increasing behavior with the inclination, which in turn produce greater critical exponents for inclined configurations.

Over fractal surfaces a critical behavior was also found. As well in this case the percolation threshold was found to change together with the exponents, but this time the relation was not so clear and the relation with the fractality of the surface could not be assess, although some promising lines were envisaged.

We have seen that for both cases, flat and fractal surfaces, the dynamics of the process is substantially affected by the geometry, and this introduces important differences in the critical behavior. That kind of changes implies that in order to get macroscopically relevant data for a possible fire spread in a given surface, it will be necessary to carefully categorize its topology. If the fractal dimension of the surface will play a role in this categorization is still an open question we hope to address in future researches.



## References

- [1] Benoit Mandelbrot, *The Fractal Geometry of Nature*, W.H. Freeman and Company, New York, 1983. ISBN:0-7167-1186-9.
- [2] Kenneth Falconer, *Fractal Geometry - Mathematical Foundations and Applications, second edition*, edited by John Wiley & Sons, 2003, Ltd ISBNs: 0-470-84861-8.
- [3] G. Albinet, G. Searby, and D. Stauffer, J. Phys. **47**, 1 (1986).
- [4] H. Téphany, J. Nahmias, and J.A.M.S. Duarte, Physica A **242**, 57 (1997).
- [5] G.L. Ball and D.P. Guertin, Int. J. Wildland Fire **2**, 47 (1992).
- [6] F.J. Barros and M.T. Mendes, Simul. Practice Theory **5**, 185 (1997).
- [7] N. Zekri, B. Porterie, J.P. Clerc, J.C. Loraud, Phys. Rev. E **71**, 046121 (2005).
- [8] B. Porterie, A. Kaiss, J.P. Clerc, N. Zekri, L. Zekri, arXiv:0805.3365v1 [physics.soc-ph]
- [9] M.E.J. Newman, D.J. Watts, Phys. Lett. A **263**, 341-346 (1999).
- [10] Various authors, *SFPE - Handbook of - Fire Protection Engineering* Published by the National Fire Protection Association, 2002.
- [11] W.E. Mell, S.L. Manzello, A. Maranghides, V International Conference on Forest Fire Research D. X. Viegas (Ed.), 2006
- [12] S.M. Dammer, H. Hinrichsen, Phys. Rev. E **68**, 016114 (2003).
- [13] F. Linder, J. Tran-Gia, S.R. Dahmen, H. Hinrichsen, arXiv:0802.1028v1 [cond-mat.stat-mech]
- [14] Jean Pierre Clerc, Internal communication (2009).
- [15] B. Porterie, N. Zekri, J.-P. Clerc, J.-C. Loraud, Combust. Flame 149, p. 63-78 (2009).
- [16] W. Mell, A. Maranghides, R. McDermott, S. Manzello, Combust. Flame, In Press, DOI:10.1016/j.combustflame.2009.06.015 (2009).

## Appendix I: SCAT Presentation

Following, the slides of the presentation of this work at the *SCAT-ALFA* Meeting at Valparaiso, Chile on July of 2009, by Dr. Andres Fuentes.

# Influence of the Fractal Landscape on the Forest Fire Propagation

**F. Aguayo, J.P. Clerc & A. Fuentes**

Polytech'Marseille

Université de Provence

IUSTI UMR 6995 du CNRS

andres.fuentes@polytech.univ-mrs.fr

SCAT-ALFA Meeting, Valparaiso Chile



## Overview

### Goal:

Introduce a real landscape (fractal) and to study the influence in the forest fire propagation

### Know-how:

The small world local network...

### To improve:

- Modeling the fractal landscape
- A representative dynamic of fire propagation behavior...

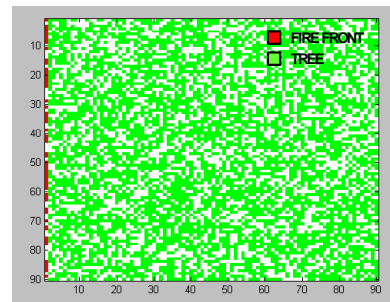


3

## Overview (Forest Fire Propagation)

### A simplified model using percolation...

- Domain  $n \times m \Rightarrow 90 \times 90$  square lattice.
- The probability that a given pixel is a tree is  $0.5 + w$  (here  $w = 0.1$ ).
- The first column of the trees is set on fire.
- The fire ignites an adjacent tree if there is one.
- The fire propagation stops when there is not any contiguous tree.



Flat landscape, homogeneous vegetation,  
the dynamic (mass loss, radiation, etc.)

4

## Overview (Forest Fire Propagation)

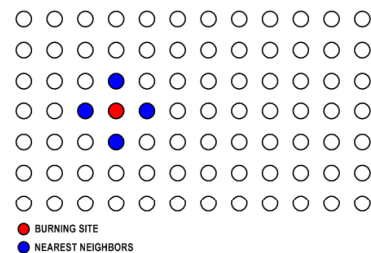
### A new approach...the Small World Network Model

[D.J. Watts and S.H. Strogatz, Nature 393, 440 (1998)]

SMALL  
WORLD  
NETWORK



REGULAR NETWORK (nearest neighbors)



## Overview (Forest Fire Propagation)

### A new approach...the Small World Network Model

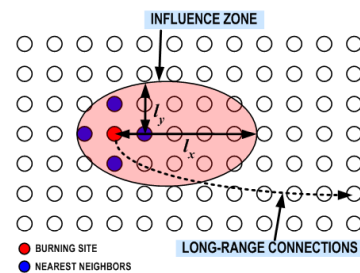
[D.J. Watts and S.H. Strogatz, Nature 393, 440 (1998)]



**Influence zone**  $\Rightarrow$  flame radiation

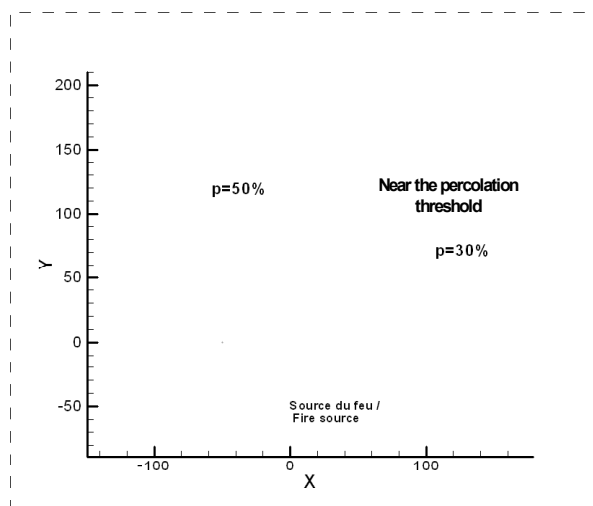
**Long-range connections**  $\Rightarrow$  firebrands

**Physics of combustion**  $\Rightarrow$  times to ignition and combustion time



## Overview (Forest Fire Propagation)

The Small World Network Model...some results of the group:



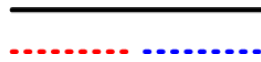
Porteire et al., Phys. Rev. E 71, 046121 (2005)

Small world effects:  
lacunarity,  
fingering,  
clustering

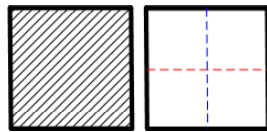
7

## Fractal dimension ( $D_f$ ) determination

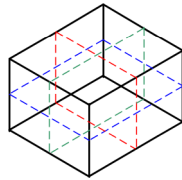
### Definition of $D_f$ :



$$2 = 2^1$$



$$4 = 2^2$$



$$8 = 2^3$$

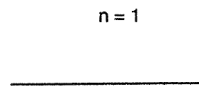
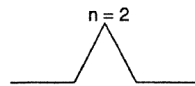
$$n = b^D$$

8

## Fractal dimension ( $D_f$ ) determination

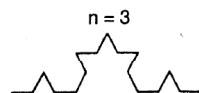
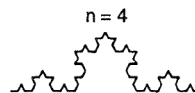
### Definition of $D_f$ :

The *Koch curve*  $\Rightarrow$  divide each line segment into three ( $b=3$ ) segments and replace the center segment with two segments the same length as the segment being replaced, and then to repeat... (Gefen 1987).


 $n = 1$ 

 $n = 2$ 

$$m = b^D$$

$$D_f = \ln(m) / \ln(b)$$


 $n = 3$ 

 $n = 4$ 

$$D_f = \ln(4) / \ln(3)$$

$$D_f \approx 1.26$$

## Fractal landscape generation

### Weierstrass Model:

$$X(x, y) = \sum_{k=1}^{\infty} C_k \lambda^{-\alpha k} \sin(\lambda^k (x \cos(B_k) + y \sin(B_k)) + A_k)$$

$A_k$  and  $B_k$ : are independent, uniformly distributed in  $[0; 2\pi)$ .

$C_k$ : are independent, normally distributed with mean 0 and variance 1.

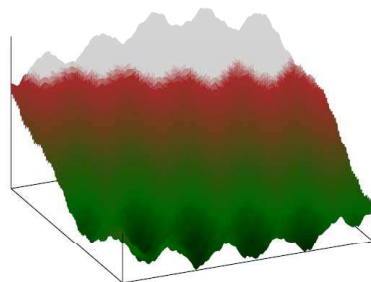
$\lambda$ : a parameter  $> 1$ .

$\alpha$ : the index of the surface.

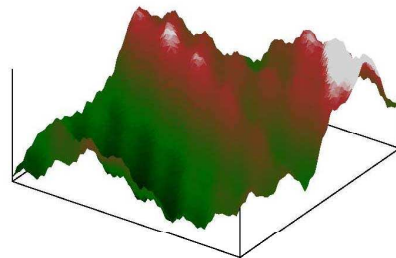
## Fractal landscape generation

### Weierstrass Model:

Some examples...



$D_f = 2.1$



$D_f = 2.2$

## Fractal dimension ( $D_f$ ) determination

### Box counting method:

In Euclidean space the volume  $V$  of an object scales as:  $V \propto L^d$   
 where  $L$  stands for the side of the object and  $d$  is its usual Euclidean dimension.

- For this we enclose the object in a cube with dimension  $d_E$
- Then we divide the side of the cube in segments of length  $\epsilon$
- The volume  $V$  will be directly proportional to the number of little cubes  $N_\epsilon$  of volume  $1/\epsilon^{d_E}$  needed to cover the object

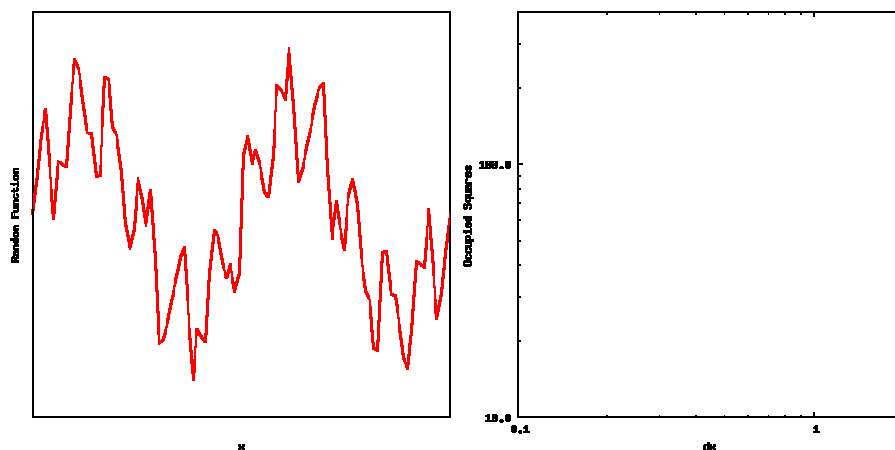
$$N_\epsilon \sim 1/\epsilon^d \text{ as}$$

$$\epsilon \rightarrow 0$$

$$d = -\lim_{\epsilon \rightarrow 0} \frac{\ln(N_\epsilon)}{\ln(\epsilon)}$$

## Fractal dimension ( $D_f$ ) determination

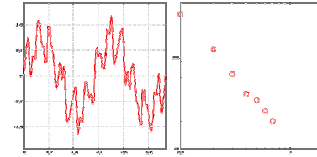
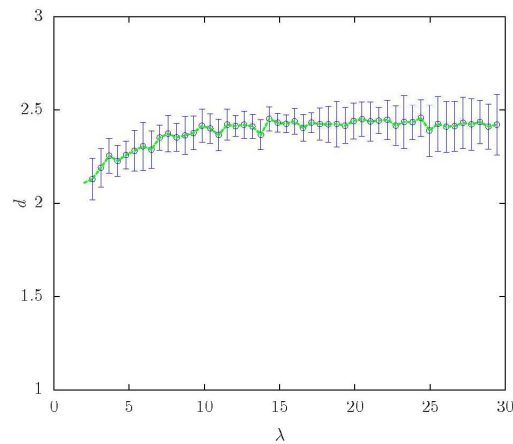
### Box counting method:





## Fractal dimension ( $D_f$ ) determination

### Box counting method in 3D:



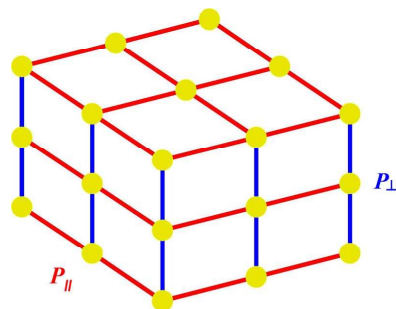
Only for given values of  $\lambda$ , the mean fractal dimension is:

$$D_f = (3 - \alpha)$$

## Additional dimension role in percolation

### Transition line:

- The bond percolation in a 2D square mesh.
- The occupancy probability  $p$  inside that mesh will be called  $p_{||}$ .
- Several of those meshes one above the other and will link the corresponding sites with a probability  $p_{\perp}$  forming a common 3D square mesh...

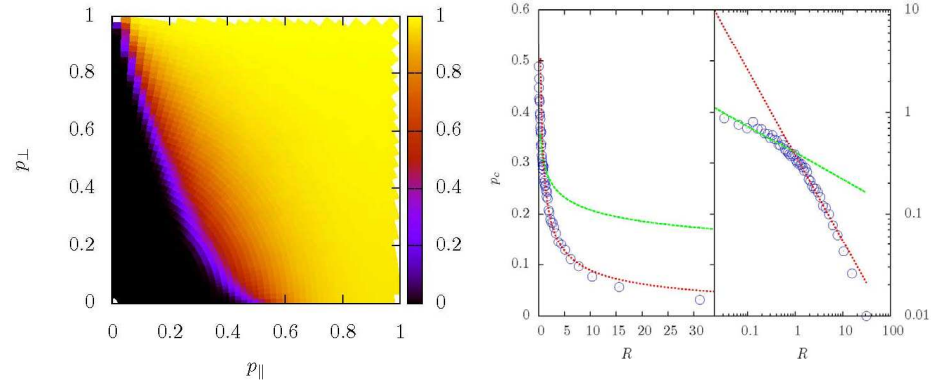


## Additional dimension role in percolation

### Transition line:

$$R = \frac{p_{\parallel}}{p_{\perp}}$$

$$p_c \propto R^{-\alpha}$$



## Dynamic propagation model

$$\frac{dC_i(t)}{dt} = C_i(t) \sum_{\langle j \rangle} \frac{dC_j(t)}{dt} W_{ij} - \Theta [C_i^{th} - C_i(t)] C_i(t) (1 - C_i(t)) U_i$$

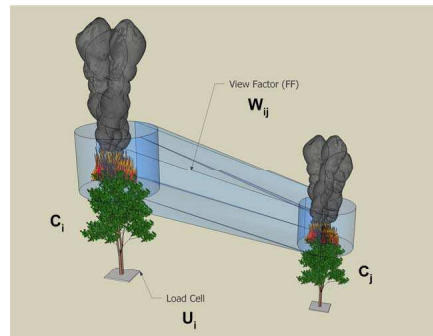
$C_i$  : the amount of fuel in the site  $i$  on time  $t$ , relative to the initial amount of fuel.

$C_i=1$  and  $C_i=0$  are stationary states of the site if no external agent is considered.

$C_i^{th}$ : the threshold linked to the ignition of the tree (time necessary to obtain a critical pyrolysis mass flux).

$U_i$  : parameter associated to mass loss when the tree is burning.

$W_{ij}$  : the interaction between trees (here proportional to radiative heat transfer).



## Dynamic propagation model

Parameters,  $U_i$ :

$$\frac{dC_i(t)}{dt} = C_i(t) \underbrace{\sum_{\langle j \rangle} \frac{dC_j(t)}{dt} W_{ij}}_{\text{without interaction} \Rightarrow W_{ij} \approx 0} - \Theta [C_i^{th} - C_i(t)] C_i(t) (1 - C_i(t)) U_i$$

without interaction  $\Rightarrow W_{ij} \approx 0$

$$\frac{dC_i(t)}{dt} = -C_i(t) (1 - C_i(t)) U_i \quad \text{With } C_i(0) = C_i^{th}$$

The analytical solution is:

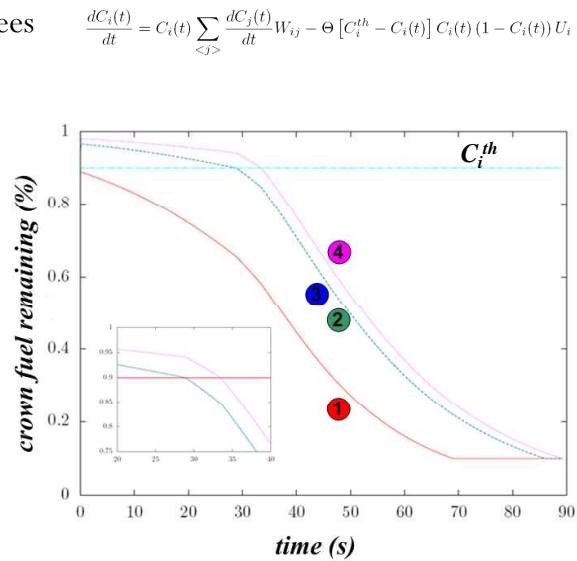
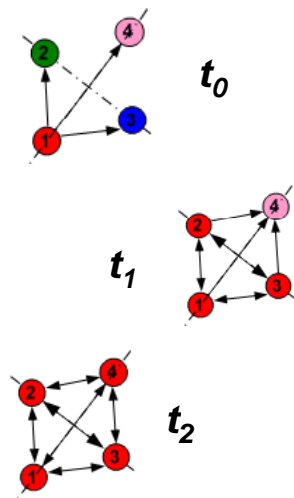
$$C_i(t) = \frac{1}{1 + \left( \frac{1}{C_i^{th}} - 1 \right) e^{U_i t}}$$

For the large times  $C_i(t) \sim A e^{-U_i t}$

$U_i$  varies as the inverse of the mean life of a tree

## Dynamics propagation model

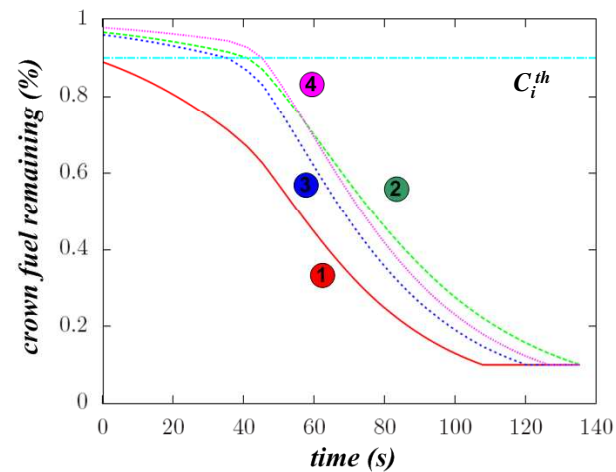
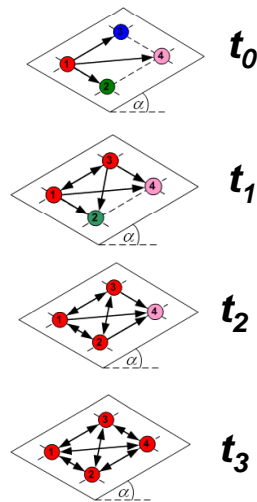
An example with only 4 trees in a flat surface:



## Dynamics propagation model

An example with only 4 trees  
in a surface with slope  $\alpha$ :

$$\frac{dC_i(t)}{dt} = C_i(t) \sum_{\langle j \rangle} \frac{dC_j(t)}{dt} W_{ij} - \Theta [C_i^{th} - C_i(t)] C_i(t) (1 - C_i(t)) U_i$$



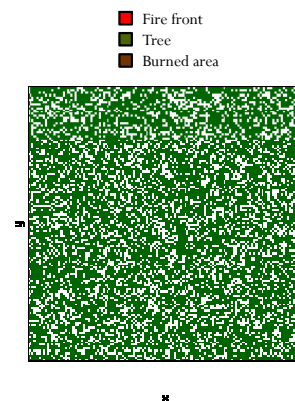
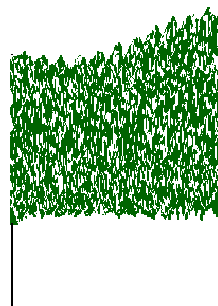
## Some results

Propagation of a forest fire in a fractal landscape:

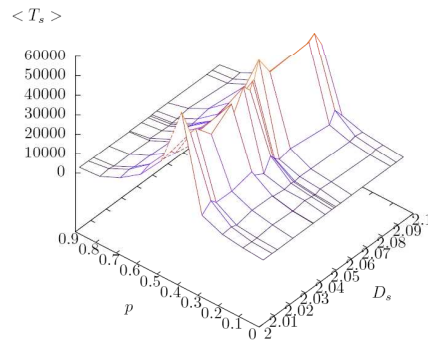
$$D_f = 2.2$$

$$\text{Doping} = 0.7$$

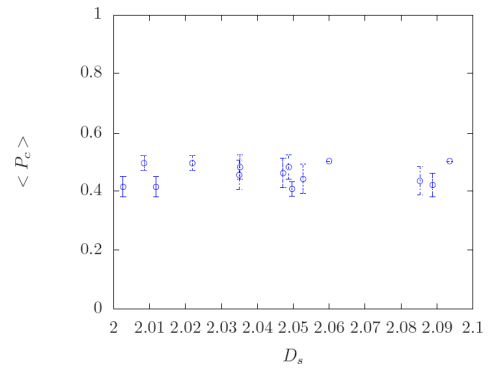
$$C_i^{th} = 0.85$$



## Some results

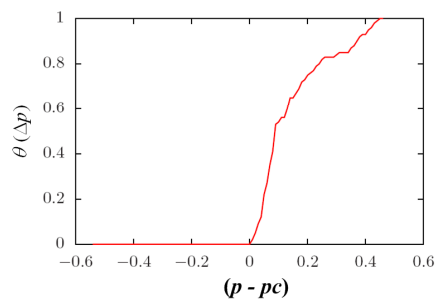


Mean time of fire  $\langle T_s \rangle$  for different surfaces  $D_s$



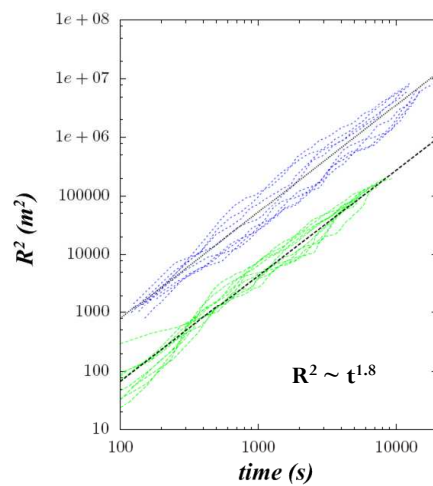
The  $P_c$  in function of  $D_s$

## Some results



$\Delta p = (p - p_c)$  :  
the distance from criticality

$\theta(\Delta p)$  : percolation probability



Critical exponent for the burned area  
in two mesh sizes

## Conclusion and perspectives

- The fractal landscape and simplified propagation model was introduced to study the influence in fire propagation front, active sites, burning area, etc...
- The effects of different type of vegetation can be considered (geometries, fuel load, ...)
- The effect of  $D_f$  in the propagation of a forest fire is being analyzed
- The universality of the phenomena is investigated now through the critical exponent.

*The presented framework could have a very interesting application in practical situations...*

**Thank you for your attention!**

*I hope that the presentation did not seem too flat considering this fractal subject...*